

20. The modified RIPA buffer was composed of 20 mM MOPS buffer, 150 mM NaCl, 1 mM EDTA, 1% NP-40, 1% deoxycholate, and 0.1% SDS; pH 7.0.
21. M.-F. Law, D. R. Lowy, I. Dvoretzky, P. M. Howley, *Proc. Natl. Acad. Sci. U.S.A.* **78**, 2727 (1981).
22. R. Treisman, U. Novak, J. Favalaro, R. Kamen, *Nature (London)* **292**, 595 (1981).
23. R. Schlegel and T. Benjamin, *Cell* **14**, 587 (1978).
24. We thank J. Bolen for performing the protein kinase assays, P. Howley for research discussions, C. Baker and P. Howley for critical reading of the manuscript,

and N. Freas for text processing. M.S.R. was supported by grant 1579 from the Council for Tobacco Research, Inc.

31 January 1986; accepted 12 May 1986

## A Synthetic Peptide from Fibronectin Inhibits Experimental Metastasis of Murine Melanoma Cells

MARTIN J. HUMPHRIES, KENNETH OLDEN, KENNETH M. YAMADA

Adhesive interactions between cells and the extracellular matrix occur at several stages of metastasis. Such interactions might be inhibited by synthetic peptide probes derived from the cell-binding regions of matrix molecules. Gly-Arg-Gly-Asp-Ser (GRGDS) is a pentapeptide sequence that appears to be critical for cell interaction with fibronectin. Coinjection of GRGDS with B16-F10 murine melanoma cells dramatically inhibited the formation of lung colonies in C57BL/6 mice. Two closely related control peptides, in which specific amino acids within the GRGDS sequence were transposed or substituted, displayed little or no activity. Inhibition by GRGDS was dose-dependent, noncytotoxic, and did not result from an impairment of cellular tumorigenicity. GRGDS may function by inhibiting tumor cell retention in the lung since radiolabeled B16-F10 tumor cells injected with the peptide were lost at a substantially greater rate than control cells.

THE COMPLEX SERIES OF EVENTS constituting tumor metastasis can be subdivided into a number of distinct steps, several of which involve the traversal of extracellular matrix barriers (1). An understanding of the interaction of metastatic cells with extracellular matrix and basement membrane components such as fibronectin and laminin (2) offers the potential for selectively interfering with a single critical step in the metastatic cascade. Preincubation or coculture of murine melanoma cells with purified laminin enhances their pulmonary colonization, whereas a proteolytic cell-binding fragment has the opposite effect (3). Despite the finding that fibronectin can help mediate the attachment of murine melanoma cells to the subendothelial matrix (4) and can promote their haptotactic migration (5), further evidence for its involvement in blood-borne metastasis is currently limited.

The ability of cells to bind fibronectin and related adhesion proteins appears to depend on a short, hydrophilic amino acid sequence, Arg-Gly-Asp-Ser, located in the cell-binding domain of the fibronectin molecule (6-9). Synthetic peptides containing this sequence act as competitive, reversible inhibitors in assays of cellular adhesion (7-12). They compete directly for fibronectin binding by cells in a noncytotoxic manner (9, 11, 13) and have been used recently to study adhesive interactions involved in platelet function (10, 11) and embryonic development (14).

Coinjection of GRGDS with  $7 \times 10^4$  B16-F10 cells resulted in a marked reduction of melanotic colonies 14 days later in the lungs of C57BL/6 mice (Fig. 1). Extending the incubation period to 21 days gave a similar degree of inhibition (Table 1). The number of visible colonies was found to

increase by approximately 50% over the extra 7 days, but the rate of appearance of new colonies was similar in both control and peptide-treated mice, indicating that the peptide did not merely retard the growth of injected cells or delay the appearance of colonies. A comparable effect has been obtained with several different batches of peptide. The inhibition by GRGDS was dose-dependent, with  $\geq 90\%$  inhibition at 3 mg per mouse. This effective concentration (3 mM, assuming a blood volume of approximately 2 ml) appears reasonable for achieving competitive inhibition of a fibronectin-related adhesive process. Previous studies in vitro often required millimolar concentrations of peptide for full inhibition (7, 9, 14), as might be expected given the low affinity of fibronectin for its receptor ( $K_d = 0.8 \times 10^{-6}M$ ) (13) and the high concentration of fibronectin in blood (0.3 g/liter) (2). In our assay system, the dosage of peptide required to completely inhibit colonization was dependent upon the number of cells injected (Table 1). At  $3 \times 10^4$  to  $5 \times 10^4$  cells injected, complete inhibition has been obtained with 3 mg of GRGDS per mouse. The reason for the decreased effectiveness of GRGDS when injected with high cell numbers is not known, although it may be related to the heterogeneity of the B16-F10 melanoma line. Substantial inhibition was observed with 3 mg of GRGDS even when  $1.5 \times 10^5$  cells were injected; the error in counting the large number of control colonies at this point may have artificially reduced the level of peptide inhibition.

Experiments routinely involved premixing of cells and peptide. However, samples in which cells and peptide were injected sequentially into separate tail veins showed a similar degree of inhibition of colonization when compared to premixed samples (Table 2,  $P = 0.2$  by *t* test adjusted by the Bonferroni correction) suggesting that preincubation had no detrimental effect on the cells. Ordinarily, extrapulmonary metastasis of B16-F10 is rare, and neither its frequency nor distribution was affected by peptide

Table 1. Effect of time of incubation and cell number injected on GRGDS inhibition of experimental metastasis. Aliquots of the indicated numbers of B16-F10 cells were injected into eight mice per sample with or without 3 mg GRGDS as described in Fig. 1A. Colony formation was examined after the incubation times shown. Six of the mice injected with  $3 \times 10^4$  cells + 3 mg of GRGDS exhibited no visible lung colonies.

Cell number ( $\times 10^{-4}$ )	Time of incubation (days)	Colony number*		Inhibition (%)
		Control	GRGDS	
7	14	69.4 $\pm$ 14.4	1.9 $\pm$ 0.8	97.3
7	21	112.4 $\pm$ 2.1	2.9 $\pm$ 0.4	97.4
3	14	8.9 $\pm$ 1.7 (8)	0.8 $\pm$ 0.5 (0)	91.0
5	14	19.9 $\pm$ 5.5 (24)	2.3 $\pm$ 1.3 (0)	88.4
10	14	136.8 $\pm$ 16.2 (136)	41.4 $\pm$ 18.2 (6)	69.7
15	14	222.6 $\pm$ 64.1 (180)	70.8 $\pm$ 28.4 (48)	68.2

\*Colony number is shown as mean  $\pm$  SE, with the median in parentheses.

M. J. Humphries and K. Olden, Howard University Cancer Center, Washington, DC 20060, and Membrane Biochemistry Section, Laboratory of Molecular Biology, National Cancer Institute, Bethesda, MD 20892. K. M. Yamada, Membrane Biochemistry Section, Laboratory of Molecular Biology, National Cancer Institute, Bethesda, MD 20892.

treatment, indicating that GRGDS did not act by altering the organ specificity of colonization. At no time has the 3 mg optimal dose of peptide been observed to cause toxicity to mice whether administered intravenously, intraperitoneally, or subcutaneously. An initial investigation of the long-term effect of a single injection of 3 mg GRGDS on mouse growth rate and survival has uncovered no deleterious effects over a period of 30 weeks.

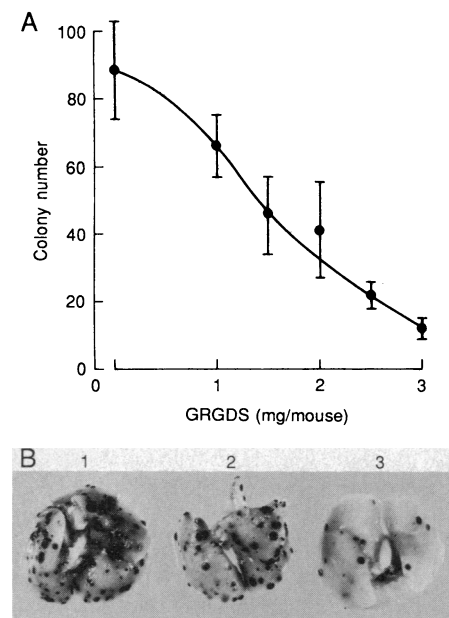


**Fig. 1.** (A) Inhibition of lung colonization by GRGDS. B16-F10 murine melanoma cells, a line selected in vivo for high lung colonization (20), were cultured as described (21). Cultures were routinely tested for microbial infection and verified to be mycoplasma-free. GRGDS (Peninsula Laboratories, Belmont, CA) was purified by Sephadex G10 chromatography in 10 mM  $\text{NH}_4\text{HCO}_3$ . The peptide was assessed as >98% pure by reversed-phase high-performance liquid chromatography analysis. The lyophilized GRGDS was then solubilized to 30 mg/ml in divalent cation-free Dulbecco's phosphate-buffered saline (PBS<sup>-</sup>; Gibco), neutralized, and sterilized by microfiltration in 0.2- $\mu\text{m}$  nylon Centrex tubes (Schleicher & Schuell). B16-F10 cells were detached for 2 minutes with 0.02% EDTA and resuspended gently to  $7 \times 10^5/\text{ml}$  in Dulbecco's MEM (DMEM; Gibco). GRGDS was then mixed with cells and 0.2-ml aliquots containing the indicated amount of peptide or PBS<sup>-</sup> and single-cell suspensions of  $7 \times 10^4$  cells were injected slowly into the lateral tail vein by the method of Fidler (22). Fourteen days later the animals were killed with ether, and their lungs were excised and fixed in 10% formaldehyde. The number of surface melanoma colonies were counted visually or with the aid of a dissecting microscope; no difference between the two procedures was detected. Extrapulmonary tumor formation was checked for each group. Control samples containing only lyophilized  $\text{NH}_4\text{HCO}_3$  did not affect colony formation. Bars represent SE ( $n = 8$ ). (B) Representative lungs from an experiment to show colonization by  $5 \times 10^4$  B16-F10 cells in controls (1) or in the presence of 1.5 and 3 mg of GRGDS (2 and 3, respectively).

Two controls were performed in order to rule out an effect of GRGDS via suppression of cellular tumorigenicity. First, groups of mice were coinjected subcutaneously with  $10^5$  B16-F10 cells with or without 3-mg GRGDS in a total volume of 0.2 ml. In all mice, actively growing tumors developed and progressed to kill their hosts at similar rates (mean killing times of 24.2 days for the control and 28.8 days for peptide-treated cells). Second, the effect of peptide treatment on growth of B16-F10 cells was examined in a standard soft-agar assay (15). Cells were preincubated at  $10^6/\text{ml}$  with GRGDS (15 mg/ml), diluted, and seeded in 0.33% agar at a final peptide concentration of 1.5 mg/ml. These pre- and coincubations mimicked conditions in the in vivo experiment described in Fig. 1A. After incubation for 6 days at 37°C, control and peptide-treated cells formed similar numbers of colonies (mean  $\pm$  SD of  $40.7 \pm 13.0\%$  and  $32.8 \pm 8.2\%$  formation, respectively). Taken together, these data indicate that GRGDS does not impair B16-F10 tumorigenicity.

Cells injected into mice were routinely monitored for viability by exclusion of trypan blue (>85%), but in addition several controls were carried out to demonstrate the noncytotoxicity of GRGDS. The possibility that preexposure to high levels of the peptide was toxic to B16-F10 cells was tested by the procedure described in Table 2. Preincubation of detached cells with GRGDS (15 mg/ml) followed by resuspension and injection in the absence of peptide resulted in a complete retention of lung colonizing activity compared to a parallel control. In a similar test, B16-F10 cells were detached, incubated with GRGDS at 15 mg/ml for up to 20 minutes, and then replated in growth medium. An indistinguishable plating efficiency was observed for all incubation times. The ability of cells to grow in soft agar in the presence of GRGDS (1.5 mg/ml) also suggests that the peptide is nontoxic, and we conclude that the inhibitory effects of GRGDS on B16-F10 pulmonary colonization cannot be explained by simple cytotoxicity.

To investigate the mechanisms responsible for GRGDS-mediated inhibition of colonization, the time course of pulmonary retention of radiolabeled B16-F10 cells was examined. As shown in Fig. 2, [ $^{125}\text{I}$ ]IUdR-labeled cells (16) were almost quantitatively recovered in the lungs 2 minutes after injection into the lateral tail vein. A significantly lower level of retention was observed when GRGDS was injected with the cells (71% versus 96%). The number of arrested cells decreased exponentially over the next 7 hours as described (16). The rate of loss was substantially higher in mice treated with

GRGDS. The time for 50% loss of cells was 160 minutes for the control and 90 minutes for cells with GRGDS. Seven hours after injection at least five times more cells remained in the lungs of control mice. This ratio increased progressively over the 2-week experimental incubation period, at the end of which it paralleled the peptide-mediated inhibition of pulmonary colonization. These results demonstrate that the primary effect of GRGDS is to accelerate the loss of arrested cells from the lung and that peptide-mediated dislodgement may be the mechanism for its inhibition of pulmonary colonization.

An early effect of GRGDS on cell detachment is also supported by mathematical analysis of these results as described by Liotta and DeLisi (17). Interference with the attachment of cells to either the endothelium or exposed endothelial basement membrane is the most likely mode of action of GRGDS, but since the process of blood-borne colonization is so complex, other mechanisms are possible. In a standard in vitro assay measuring the degree of cell spreading on immobilized fibronectin, GRGDS markedly inhibited the adhesion of

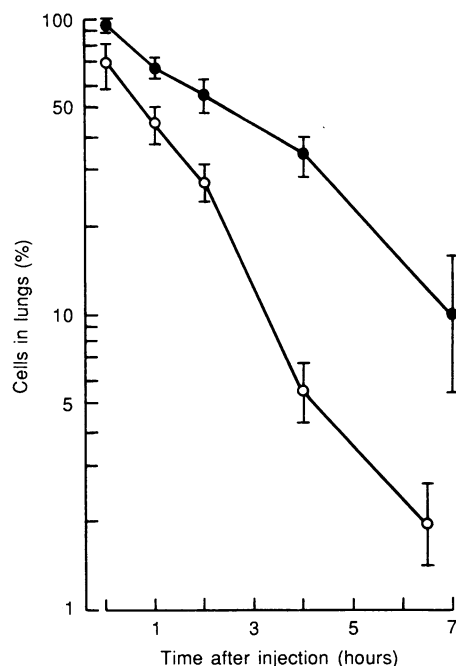


**Fig. 2.** Effect of GRGDS on pulmonary retention of B16-F10 cells. Cells were plated at  $2 \times 10^6$  per 75-cm<sup>2</sup> flask and the next day were labeled with [ $^{125}\text{I}$ ]IUdR (0.4  $\mu\text{Ci}/\text{ml}$ , 200  $\mu\text{Ci}/\text{mmol}$ ; New England Nuclear) for 24 hours in growth medium (16). Cells were then detached as described (Fig. 1A) and  $5 \times 10^4$  cells were injected with or without 3 mg GRGDS into the lateral tail vein of C57BL/6 mice. At the indicated times, mice were sacrificed by cervical dislocation, and the lungs were excised and exsanguinated in 70% ethanol (16) before counting for radioactivity. Bars represent SD ( $n = 4$ ).

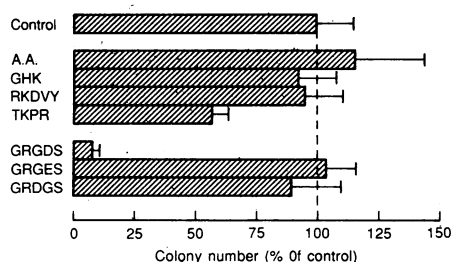


Fig. 3. Specificity of the inhibition of lung colonization by GRGDS. GRGDS, GRGES, and GRDGS were purchased from Peninsula Laboratories; TKPR, RKDVY, and GHK were from Bachem (Torrance, CA); and the free amino acids Gly, L-Arg, L-Asp, and L-Ser were from Sigma (St. Louis, MO). All peptides were purified and solubilized as described (Fig. 1A). Groups of seven or eight mice were injected with 0.2-ml aliquots of  $10^5$  B16-F10 cells together with 6  $\mu$ mol of each peptide or with free amino acids equivalent to 6  $\mu$ mol GRGDS (3 mg GRGDS = 6  $\mu$ mol). Results are expressed as percentage of the mean of the control, which was 251 colonies per mouse in this experiment.  $P = 0.2$  for TKPR and  $<0.002$  for GRGDS as measured by Welch's modification to the Student's  $t$  test. Error bars represent the SE.

B16-F10 cells at a concentration of 500  $\mu$ g/ml (Table 3). Peptide-mediated inhibition of spreading was completely reversed by gentle washing and reincubation of rounded cells in peptide-free medium (Table 3), indicating that the effect of GRGDS was not due to cytotoxicity. Thus, GRGDS is able to disrupt the adhesion of B16-F10 cells in vitro.

The extent of tumor-cell arrest can be greatly influenced by the presence of homo- or heterotypic cell clumps (18), and it is therefore conceivable that GRGDS could act by inhibiting embolus formation. Over the time frame used for injection of mice, no aggregation of B16-F10 cells was observed (suspensions consisted of  $>98\%$  single cells with no clumps larger than paired cells). This finding rules out an artifactual effect of the peptide prior to injection, a conclusion supported by the finding that sequential injection of cells and peptide was as effective as premixing and that preincubation of cells with GRGDS followed by washing and resuspension in the absence of peptide did not inhibit their colonizing potential (Table 2).

In order to investigate the specificity of the GRGDS effect, a series of peptides as well as the free amino acids were tested in equimolar amounts in the B16-F10 lung colonization assay (Fig. 3). The peptides included three hydrophilic sequences unrelated to GRGDS, Gly-His-Lys (GHK), Thr-Lys-Pro-Arg (TKPR, tuftsin) and Arg-Lys-Asp-Val-Tyr (RKDVY, a peptide from thymopoietin), and two synthetic molecules homologous to the GRGDS sequence, Gly-

Arg-Gly-Glu-Ser (GRGES) and Gly-Arg-Asp-Gly-Ser (GRDGS). Both GRGES (in which Asp is conservatively substituted by Glu) and GRDGS (in which the central Gly and Asp residues are transposed) are inactive in cell adhesion assays (8), thereby providing evidence for the specificity of the GRGDS inhibition.

Inhibition by GRGDS was statistically significant ( $P < 0.002$ ). Both GHK- and RKDVY-treated cells formed similar numbers of lung colonies as the control. The modest inhibition obtained with tuftsin (TKPR) was not statistically significant ( $P = 0.2$ ). It is possible that this limited effect, if real, is a reflection of the known ability of tuftsin to stimulate killing of tumor cells by the immune system (19). The lack of inhibition of colonization by unrelated peptides suggests that a nonspecific effect of any hydrophilic peptide is unlikely to explain GRGDS-mediated inhibition. Similarly, coinjection of an equimolar mixture of Gly, Arg, Asp, and Ser showed a complete lack of activity, indicating that the effect was not an artifact caused by the particular molar composition of amino acids in GRGDS (Fig. 3).

Neither GRDGS nor GRGES caused significant inhibition of pulmonary colonization (Fig. 3). The fact that relatively minimal changes within the GRGDS peptide,

Table 2. Effect of injection protocol and preexposure on inhibition of metastasis by GRGDS. To study the effect of the injection protocol,  $7 \times 10^4$  B16-F10 cells were injected with or without premixing with 3 mg of GRGDS as described (Fig. 1A) or were administered sequentially by a dual injection into both lateral tail veins without premixing. Colony formation was examined 14 days later. To study the toxicity of GRGDS B16-F10 cells, detached as described (in the legend to Fig. 1A), were treated with either GRGDS (15 mg/ml; final concentration 3 mg per mouse) or an equivalent volume of divalent cation-free Dulbecco's phosphate-buffered saline (PBS<sup>-</sup>) for 5 minutes at room temperature. For the "resuspension in growth medium" protocol, cells were centrifuged and resuspended to  $5 \times 10^5$  per milliliter with Dulbecco's modified Eagle's medium in the absence of GRGDS. For both protocols, 0.2-ml aliquots of these mixtures were then injected into mice and the mice were examined for pulmonary colonization 14 days later.

Treatment	Colony number (mean $\pm$ SE)	
	Control	GRGDS
<i>Injection protocol</i>		
PBS <sup>-</sup>	97.7 $\pm$ 14.4	
Premixed		11.9 $\pm$ 2.5
Dual injection		18.7 $\pm$ 3.4
<i>Reversibility</i>		
No resuspension	113 $\pm$ 22.3	12.3 $\pm$ 6.0
Resuspension in growth medium	71.9 $\pm$ 28.8	136 $\pm$ 43.0

Table 3. Reversibility of GRGDS inhibition of B16-F10 spreading on fibronectin. The effect of GRGDS (500  $\mu$ g/ml) on the spreading of B16-F10 cells on immobilized fibronectin (5  $\mu$ g/ml) was examined as described previously (8).

Treatment*	Spreading (%)	
	1	2
PBS <sup>+</sup> (30)	69.0 $\pm$ 3.2	
GRGDS (30)	4.5 $\pm$ 1.7	
PBS <sup>+</sup> (90)	77.3 $\pm$ 3.9	
GRGDS (90)	7.0 $\pm$ 2.6	
PBS <sup>+</sup> (30)	PBS <sup>+</sup> (60)	79.5 $\pm$ 6.2
GRGDS (30)	PBS <sup>+</sup> (60)	77.8 $\pm$ 1.0

\*The duration of treatment in minutes is shown in parentheses. Treatments 1 and 2 were separated by gentle washing.

such as transposition of two amino acids within an otherwise identical peptide or conservative substitution of a single amino acid of identical charge (Glu for Asp), has such a dramatic effect on activity illustrates a striking specificity for the GRGDS sequence. These data reinforce the conclusion drawn from lung-retention data (Fig. 2) that GRGDS inhibits lung colonization through its ability to interfere with cellular adhesive processes.

The exact mechanism of GRGDS-mediated inhibition remains to be determined, but likely possibilities include peptide disruption of cell attachment or interference with cell migration during invasion. The use of specific, competitive peptide inhibitors of cell adhesion and migration (that can be manufactured and purified in large quantities) could theoretically provide a rational basis for therapy of disorders involving aberrant adhesion or invasion, such as in the prevention of metastatic seeding of cancer cells after surgical removal of a primary tumor.

#### REFERENCES AND NOTES

1. I. J. Fidler, D. M. Gersten, I. R. Hart, *Adv. Cancer Res.* **28**, 149 (1978); G. Poste and I. J. Fidler, *Nature (London)* **283**, 139 (1980); G. L. Nicolson, *Biochim. Biophys. Acta* **695**, 113 (1982); L. A. Liotta, C. N. Rao, S. H. Barsky, *Lab. Invest.* **49**, 636 (1983); J. B. McCarthy et al., *Cancer Metastasis Rev.* **4**, 125 (1985).
2. E. D. Hay, Ed., *Cell Biology of Extracellular Matrix* (Plenum, New York, 1981); K. M. Yamada, *Annu. Rev. Biochem.* **52**, 761 (1983); R. L. Trelstad, Ed., *The Role of Extracellular Matrix in Development* (Liss, New York, 1984); R. O. Hynes, *Annu. Rev. Cell Biol.* **1**, 67 (1985).
3. S. H. Barsky et al., *J. Clin. Invest.* **74**, 843 (1984); V. P. Terranova et al., *Science* **226**, 982 (1984).
4. G. L. Nicolson et al., *Exp. Cell Res.* **135**, 461 (1981).
5. J. Lacovara, E. B. Cramer, J. P. Quigley, *Cancer Res.* **44**, 1657 (1984); J. B. McCarthy and L. T. Furcht, *J. Cell Biol.* **98**, 1474 (1984).
6. M. D. Pierschbacher, E. G. Hayman, E. Ruoslahti, *Proc. Natl. Acad. Sci. U.S.A.* **80**, 1224 (1983).
7. M. D. Pierschbacher and E. Ruoslahti, *Nature (London)* **309**, 30 (1984); K. M. Yamada and D. W. Kennedy, *J. Cell Biol.* **99**, 29 (1984); M. D. Pierschbacher and E. Ruoslahti, *Proc. Natl. Acad. Sci. U.S.A.* **81**, 5985 (1984).

8. K. M. Yamada and D. W. Kennedy, *J. Cell. Biochem.* **28**, 99 (1985).
9. S. K. Akiyama and K. M. Yamada, *J. Biol. Chem.* **260**, 10402 (1985).
10. C. R. Ill, E. Engvall, E. Ruoslahti, *J. Cell Biol.* **99**, 2140 (1984).
11. M. Ginsberg *et al.*, *J. Biol. Chem.* **260**, 3931 (1985); D. M. Haverstick *et al.*, *Blood* **66**, 496 (1985).
12. E. G. Hayman, M. D. Pierschbacher, E. Ruoslahti, *J. Cell Biol.* **100**, 1948 (1985).
13. S. K. Akiyama and K. M. Yamada, *J. Biol. Chem.* **260**, 4492 (1985).
14. J. -C. Boucaut *et al.*, *J. Cell Biol.* **99**, 1822 (1984).
15. K. Nagata and Y. Ichikawa, *J. Cell. Physiol.* **98**, 167 (1979).
16. I. J. Fidler, *J. Natl. Cancer Inst.* **45**, 773 (1970).
17. L. A. Liotta and C. DeLisi, *Cancer Res.* **37**, 4003 (1977).
18. I. J. Fidler, *Eur. J. Cancer* **9**, 223 (1973); L. A. Liotta, J. Kleinerman, G. M. Saidel, *Cancer Res.* **36**, 889 (1976); G. T. Gasic, *Cancer Metastasis Rev.* **3**, 99 (1984).
19. V. A. Najjar and M. Fridkin, Eds., *Ann. N.Y. Acad. Sci.* **419**, 1 (1983).
20. I. J. Fidler, *Nature (London) New Biol.* **242**, 148 (1973).
21. ———, *Cancer Res.* **34**, 1074 (1974).
22. ———, *Methods Cancer Res.* **15**, 399 (1978).
23. We thank I. J. Fidler of the M. D. Anderson Hospital, University of Texas, Houston, TX, for providing B16-F10 cells. Supported in part by grant CA-34918 from the U.S. Public Health Service to K. Olden.

2 October 1985; accepted 19 May 1986

## A Wind-Forced Ekman Spiral as a Good Statistical Fit to Low-Frequency Currents in a Coastal Strait

MICHAEL W. STACEY, STEPHEN POND, PAUL H. LEBLOND

Ekman's classical analysis of wind-driven currents is a fundamental component of the modern circulation theory of the oceans, but there have been few good observations of the predicted Ekman spiral, where the velocity vector rotates clockwise in direction (in the Northern Hemisphere) and decays exponentially in magnitude with increasing depth. An analysis of recent cyclesonde velocity measurements based on the use of empirical orthogonal functions, however, suggests that a classical Ekman spiral was a good statistical fit to a significant portion of the low-frequency current fluctuations in the Strait of Georgia, British Columbia, for fluctuation periods of about 5 to 10 days.

THE RESPONSE OF THE OCEAN TO the forcing of the wind was first analyzed theoretically in 1905 by Ekman (1), who assumed (i) an infinitely wide, steady-state ocean with no horizontal variations and (ii) a constant eddy viscosity to distribute momentum into the water column. The basic predictions of the analysis, that the surface current veers to the right of the wind (in the Northern Hemisphere) and decreases in amplitude with depth, are gen-

erally accepted, but, because of the assumptions and a lack of reliable observations (2), the details generally are not. An empirical orthogonal function analysis of the low-frequency current fluctuations at a cyclesonde, that is, a profiling current meter, moored in the Strait of Georgia, British Columbia, however, suggests that during the observation period a classical Ekman spiral was an accurate representation of much of the actual flow field. To our knowl-

edge, the results described here are the most supportive of any to date of Ekman's simple theory, particularly because they apply to an ensemble of realizations, taken over a period of several months, and because they show a good fit to the vertical variation in the horizontal currents over a depth of over 100 m.

The locations of the cyclesonde mooring and the anemometer station are shown in Fig. 1. Deployed from 20 June 1984 until 14 January 1985, the cyclesonde was set to profile to within 20 m of the surface and to a depth of 300 m in a total water depth of 370 m. These data allowed the synthesis of 15 discrete velocity time series at 20-m intervals (3). The east-west and north-south velocity components of the currents and the wind were low-pass filtered by applying a 25-hour running mean three times successively. The filter passes approximately 80% of the amplitude at 0.2 cycle per day, approximately 95% at 0.1 cycle per day. The filtered time series were then resampled at 6-hour intervals. Autospectra of the filtered currents showed that the dominant periods of the fluctuations were greater than 5 days.

Two-dimensional, that is, complex empirical orthogonal, functions (4) were calculated from the current velocity time series (with the mean removed). Figure 2 shows the variance accounted for by the first three orthogonal modes as a function of depth. The first three modes together account for 89% of the total variance. Mode 1 dominates the variance from 20 to 160 m. Figure 3 shows the mode 1 eigenfunction. The dots in Fig. 3 locate the tips of the orthogonal, horizontal velocity vectors ( $U$ ,  $V$ ) of a classical Ekman spiral, given by

$$U = V_0 \cos \left( \frac{\pi}{4} + \frac{\pi z}{D_E} \right) \exp \left( \frac{\pi z}{D_E} \right)$$

$$V = V_0 \sin \left( \frac{\pi}{4} + \frac{\pi z}{D_E} \right) \exp \left( \frac{\pi z}{D_E} \right)$$

where the  $z$ -axis is directed upward and equals zero at the ocean's surface (5).  $U$  and

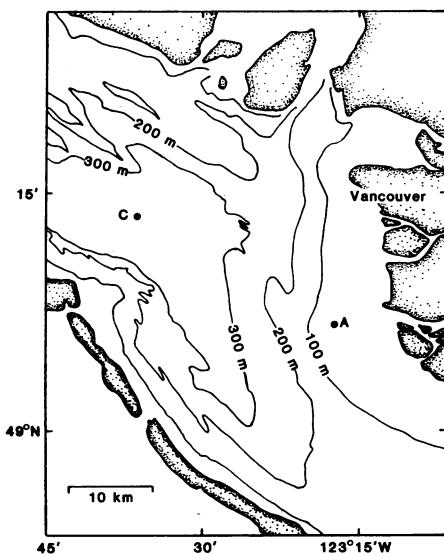


Fig. 1. Plan view of the Strait of Georgia, showing the cyclesonde (C) and anemometer (A) stations. The anemometer is located 18 m above sea level.

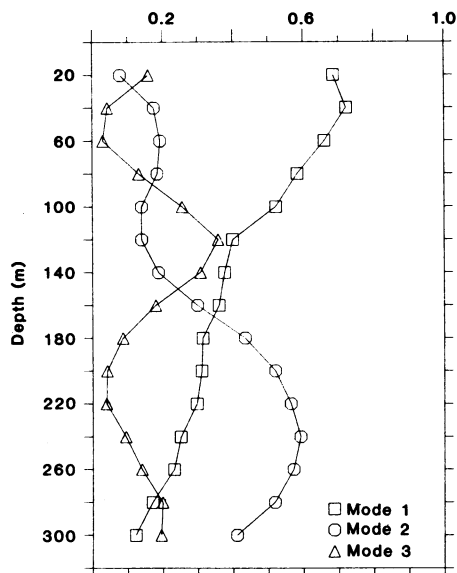


Fig. 2. The fraction of the variance explained by the first three orthogonal modes as a function of depth.

Department of Oceanography, University of British Columbia, Vancouver, British Columbia, Canada V6T 1W5.



**A synthetic peptide from fibronectin inhibits experimental metastasis of murine melanoma cells**

MJ Humphries, K Olden and KM Yamada (July 25, 1986)

*Science* **233** (4762), 467-470. [doi: 10.1126/science.3726541]

Editor's Summary

---

This copy is for your personal, non-commercial use only.

---

- Article Tools** Visit the online version of this article to access the personalization and article tools:  
<http://science.sciencemag.org/content/233/4762/467>
- Permissions** Obtain information about reproducing this article:  
<http://www.sciencemag.org/about/permissions.dtl>

*Science* (print ISSN 0036-8075; online ISSN 1095-9203) is published weekly, except the last week in December, by the American Association for the Advancement of Science, 1200 New York Avenue NW, Washington, DC 20005. Copyright 2016 by the American Association for the Advancement of Science; all rights reserved. The title *Science* is a registered trademark of AAAS.